AD-A226 870

Solar Cycle Effects on the Near-Earth Plasmas and Space Systems

Prepared by

D. J. GORNEY
Space Sciences Laboratory
Laboratory Operations
The Aerospace Corporation
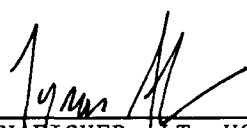El Segundo, CA 90245-4691

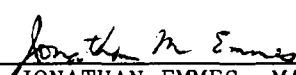6 August 1990

Prepared for

DTIC
ELECTE
SEP 28 1990
S B D

This report was submitted by The Aerospace Corporation, El Segundo, CA 90245, under Contract No. F04701-88-C-0089 with the Space Systems Division, P. O. Box 92960, Los Angeles, CA 90009-2960. It was reviewed and approved for The Aerospace Corporation by A. B. Christensen, Director, Space Sciences Laboratory.

Lt. T. Fisher was the project officer for the Mission–Oriented Investigation and Experimentation (MOIE) Program.

This report has been reviewed by the Public Affairs Office (PAS) and is releasable to the National Technical Information Service (NTIS). At NTIS, it will be available to the general public, including foreign nationals.

This technical report has been reviewed and is approved for publication. Publication of this report does not constitute Air Force approval of the report's findings or conclusions. It is published only for the exchange and stimulation of ideas.

TRYON FISHER, 1LT, USAF
MOIE Project Officer
SSD/CLPO

JONATHAN EMMES, MAJ, USAF
MOIE Program Manager
AFSTC/WCO OL-AB

REPORT DOCUMENTATION PAGE

1a. REPORT SECURITY CLASSIFICATION Unclassified			1b. RESTRICTIVE MARKINGS		
2a. SECURITY CLASSIFICATION AUTHORITY			3. DISTRIBUTION/AVAILABILITY OF REPORT Approved for public release; distribution unlimited		
2b. DECLASSIFICATION/DOWNGRADING SCHEDULE					
4. PERFORMING ORGANIZATION REPORT NUMBER(S) TR–0089(4940–06)–3			5. MONITORING ORGANIZATION REPORT NUMBER(S) SSD–TR–90–23		
6a. NAME OF PERFORMING ORGANIZATION The Aerospace Corporation Laboratory Operations		6b. OFFICE SYMBOL (If applicable)	7a. NAME OF MONITORING ORGANIZATION Space Systems Division		
6c. ADDRESS (City, State, and ZIP Code) El Segundo, CA 9024–4691			7b. ADDRESS (City, State, and ZIP Code) Los Angeles Air Force Base Los Angeles, CA 90009–2960		
8a. NAME OF FUNDING/SPONSORING ORGANIZATION		8b. OFFICE SYMBOL (If applicable)	9. PROCUREMENT INSTRUMENT IDENTIFICATION NUMBER F04701–88–C–0089		
8c. ADDRESS (City, State, and ZIP Code)			10. SOURCE OF FUNDING NUMBERS		
			PROGRAM ELEMENT NO.	PROJECT NO.	TASK NO.	WORK UNIT ACCESSION NO.

11. TITLE (Include Security Classification)
Solar Cycle Effects on Near-Earth Plasmas and Space Systems

12. PERSONAL AUTHOR(S)
Gorney, David J.

13a. TYPE OF REPORT	13b. TIME COVERED FROM _____ TO _____	14. DATE OF REPORT (Year, Month, Day) 1990 August 06	15. PAGE COUNT 40

16. SUPPLEMENTARY NOTATION

17.	COSATI CODES		18. SUBJECT TERMS (Continue on reverse if necessary and identify by block number)
FIELD	GROUP	SUB-GROUP	Solar activity Magnetosphere
			Satellite Communications Ionosphere

19. ABSTRACT (Continue on reverse if necessary and identify by block number)

Recently, solar physicists have predicted with ever-increasing confidence that the upcoming maximum of solar activity, scheduled to occur near 1990, might be the most extreme ever recorded. It seems certain, based on the observed rate of increase in solar activity starting with the most recent minimum in 1986, that the upcoming solar maximum will be the most severe of those which have occurred during the "space age". Correlations between solar activity and disturbances in the near-earth magnetospheric and ionospheric plasmas which adversely affect communications and space systems are well documented. The implementation of larger, more complex (and perhaps more susceptible) space systems over the last decade, at a time when the space environment might begin to demonstrate its most hostile nature, has led to concern and speculation about the expected performance and survivability of these space systems over the next decade. Unfortunately, because of the complex and sometimes indirect interactions between the sun and the plasma environment in near-earth space, very few firm quantitative predictions can be made regarding the expected effects of an extreme solar maximum on the near-earth environment or on the complex systems operating in that environment. However, a number of qualitative predictions can be made with high confidence. Satellite communications links in the VHF/UHF range will suffer signal

20. DISTRIBUTION/AVAILABILITY OF ABSTRACT [X] UNCLASSIFIED/UNLIMITED ☐ SAME AS RPT. ☐ DTIC USERS	21. ABSTRACT SECURITY CLASSIFICATION Unclassified	
22a. NAME OF RESPONSIBLE INDIVIDUAL	22b. TELEPHONE (Include Area Code)	22c. OFFICE SYMBOL

DD FORM 1473, 84 MAR 83 APR edition may be used until exhausted. SECURITY CLASSIFICATION OF THIS PAGE
All other editions are obsolete
UNCLASSIFIED

19. ABSTRACT (continued)

fades more often and with greater severity. Short wave and airline communications will be sporadically disrupted. Satellites will experience electrical charging of their surface and internal dielectric components, resulting in disruptive electrostatic discharges (ESDs), and micro-electronic devices on satellites will experience upsets more often. The purpose of this report is to review the direct and indirect influences of solar activity on the near-earth plasma environment and on systems which operate within that environment.

Accession For

NTIS GRA&I	☑
DTIC TAB	☐
Unannounced	☐
Justification	

By

Distribution/

Availability Codes

Dist	Avail and/or Special
A-1	

CONTENTS

FIGURES

1. INTRODUCTION

The regular variation of solar activity, which has come to be known as the 11-year sunspot cycle, was discovered in the mid-19th century[1,2], although documented scientific observations of its existence extend as far back as the 17th century[3,4]. Perhaps the earliest recorded physical effects of solar activity on man were intermittent telegraph outages[5] in the late 1850's. More recently, a large geomagnetic storm in 1956 severely impaired the operation of the first transatlantic voice cable, and a cable system in the midwestern U.S. was shut down temporarily by geomagnetic effects as recently as 1972. Throughout history, many soothsayers must have been influenced by solar-produced "omens" such as dramatic visual auroral displays in the night sky. and perhaps many influential political or military messages were disrupted when carrier pigeons lost their way due to confusing magnetic signals during active solar conditions; but the author will refrain from discussing these speculations further even though their effect on human destiny might well overshadow the effects on modern systems. Recently, solar physicists have predicted with ever-increasing confidence that the upcoming maximum of solar activity, scheduled to occur near 1990, might be the most extreme ever recorded[6-10]. It seems certain, based on the observed rate of increase in solar activity starting with the most recent minimum[10] in 1986 (solar cycle 22), that the upcoming solar maximum will be the most severe of those which have occurred during the "space age" (i.e., solar cycles 20-22).

Correlations between solar activity and disturbances in the near-earth magnetospheric and ionospheric plasmas which adversely affect communications and space systems are well documented. The implementation of larger, more complex (and perhaps more susceptible) space systems over the last decade, at a time when the space environment might begin to demonstrate its most hostile nature, has led to concern and speculation about the expected performance and survivability of these space systems over the next decade. Unfortunately, because of the complex and sometimes indirect interactions between the sun and the plasma environment in near-earth space,[11,12] very few firm quantitative predictions can be made regarding the expected effects of an extreme solar maximum on the near-earth environment or on the complex systems operating in that environment. However, a number of qualitative predictions can be made with high confidence. Satellite communications links in the VHF/UHF range will suffer signal fades and phase scintillation more often and with greater severity[13] (e.g., > 20 dB). Shortwave and airline communications will be sporadically disrupted, especially over the polar regions. Disruptions may occur in electrical power distribution systems on the ground. Satellites will experience increased levels of electrical charging of their surface and internal dielectric components, resulting in disruptive or even damaging electrostatic discharges (ESDs). Microelectronic devices on satellites (and to a lesser extent, high-flying aircraft) will experience logic upsets more often.

The purpose of this report is to review the direct and indirect influences of solar activity on the near-earth plasma environment and on systems which operate within that environment. The review concentrates on those major areas where our current physical understanding of these

interactions can lead to firm predictions of the expected effects of an extreme solar maximum on the near-earth plasma environment.

This report is divided into four sections, including the introduction. The following section describes the near-earth plasma environment, including the ionosphere and magnetosphere. The physically and operationally critical characteristics of the magnetosphere/ionosphere system are identified, showing how these characteristics are driven by solar activity. The effects of disturbances in the magnetosphere/ionosphere system on the performance and survivability of communications and space systems is also described. The third section describes how various characteristics of the sun vary over the solar activity cycle and how these variations transform into solar-terrestrial effects. An effort is made to distinguish direct from indirect effects, and to indicate which effects are physically well-understood (and perhaps predictable) and which are understood only synoptically. The final section offers a summary, and is intended to address the general question: What if solar cycle 22 is the largest ever?

2. THE INFLUENCE OF SOLAR ACTIVITY ON THE IONOSPHERE AND MAGNETOSPHERE

Man-made electrical, satellite, and communications systems are strongly affected by the near-earth plasma environments which comprise the ionospheric and magnetospheric regions. Plasmas within the ionosphere, at altitudes from 50 - 500 km, arise from the ionization of neutral atmospheric atoms and molecules by solar illumination and by the precipitation of energetic charged particles (ions and electrons) from space. Plasmas in the magnetospheric region are comprised of ions and electrons which are energized, distributed, and confined out to distances of several earth diameters by complex dynamical interactions between the earth's own dipole magnetic field, the ionosphere, and the magnetized solar wind. Thus, the sun (including its light output, its magnetic configuration, and its output of solar wind), the magnetosphere, the ionosphere, and the atmosphere are a coupled physical system, whose responses to changes in solar activity are pervasive and complex. Individual man-made systems typically interact with a very small segment of this coupled system, and it can be very difficult to draw a straight line between cause and effect when anomalous conditions occur. The goal of this section is to summarize the major cause-and-effect relationships between solar activity and conditions in the ionosphere and magnetosphere.

The earth's ionosphere is a (relatively) thin layer of partially ionized, magnetized plasma. Typical plasma densities in the ionosphere[14] range from $10^3 - 10^6$ cm^{-3}, compared to neutral densities of about $10^7 - 10^{16}$ cm^{-3}. Because of the strong coupling between the ionosphere and the sun, atmosphere, and magnetosphere, the phenomenology of the ionosphere is complex and has been under scientific examination for many years. In order to categorize the various physical processes which govern ionospheric structure, one must subdivide the ionosphere into at least two or three layers in altitude, two or three zones in latitude, and consider the day and night ionosphere separately. No attempt will be made here to review all the fundamentals of ionospheric physics for each of these regions, but it is necessary to point out some of the key relationships between solar activity and ionospheric structure.

By far the most important subdivision of the ionosphere, especially at equatorial and midlatitudes, is that between day and night. During the day, the most important ionizing agent is direct solar illumination at ultraviolet (UV) wavelengths, which contributes an average ionizing energy flux of about 5 erg/cm^2-sec. Photoionization balances collisional recombination in the E (90–120 km altitude) and F_1 (~250 km) regions of the ionosphere, with peak steady-state ionization densities typically occurring in the 250–400 km altitude range. The peak ionization density and the total column electron content (TEC) of the ionosphere responds directly and abruptly to variations in the solar UV radiation, and ~ 100% changes in these quantities can occur essentially without warning during severe solar flare conditions[15]. Ultimately, the peak ionization density controls the maximum radio frequency which will execute multiple-hop ray paths, and TEC affects frequency management and range corrections for transionospheric communications, tracking, and navigational signals. The critical transmission frequencies of the iono-

sphere, corresponding to peak ionization densities in the E and F regions, are called the f_oE and f_oF_1 frequencies. The ionospheric critical frequencies are important for frequency management of over–the–horizon radio and radar systems. These frequencies can vary from 1–3 MHz in quiet solar conditions to > 15 MHz in very active conditions. Navigational range errors caused by the effects of TEC variations on space–based radio beacon transmissions are usually small, but can be important for the most critical applications. At night the solar–induced ionization densities collapse rapidly (in seconds at low altitudes and in a few hours at higher altitudes). This rapid collapse, along with dynamic effects near the dusk terminator, lead to the development of ionization plumes and irregularities which also affect radio–frequency propagation in the dusk–midnight local time sector[13].

The D region of the ionosphere, at about 80 km altitude, also experiences abrupt and direct effects of solar activity. Solar flare x rays and relativistic protons arrive at the earth within minutes of the occurrence of a solar flare. This radiation can penetrate into the ionospheric D region and momentarily can become the dominant ionization source there. The solar flare protons generally gain access to the earth at high latitudes only, but can cause measurable increases in D region ionization. These effects can be observed as increases in the absorption of cosmic radio noise, and the occurrences are called polar cap absorption (PCA) events. At times, fluxes of relativistic electrons from interplanetary space can have significant effects on the ionospheric D region. While the source of the relativistic electrons is not thoroughly understood, the events do show a (inverse) dependence on the solar cycle[16]. The D region events can cause disruption of short–wave and airline communications, and can have deleterious effects on other reconnaissance systems.

At high latitudes, the precipitation of energetic ions and electrons from the magnetosphere and ionosphere (the same particles which are responsible for stimulating the visible–light emissions in auroral displays) is the dominant ionization source. The magnitude of the precipitating particle flux varies enormously, from less than one to several hundred erg/cm^2-sec. The magnitude of the precipitation is directly correlated with the occurrence of geomagnetic "events" called storms and substorms which can last from several minutes to several days. The occurrence of geomagnetic activity is caused by a complex set of interactions between the solar wind and the magnetosphere, discussed in more detail later in this section. During these events, ionospheric parameters such as f_oE, f_oF_2, and TEC can vary dramatically and can develop strong localized horizontal gradients. The auroral zone is also the primary location for the development of small–scale time–varying ionization irregularities which can cause severe phase and amplitude scintillations (i.e., fades) at HF, VHF, and UHF.

During auroral events, strong electrical currents flow through the high–conductance channels in the ionosphere caused by localized ionization enhancements. These regions experience resistive or joule heating which can have consequences for the energy balance of the neutral atmosphere (global joule dissipation rates as high as a terawatt are possible). As a result of enhanced joule heating, "bulges" can develop in the neutral atmosphere above ~ 100 km, affecting the trajectories of low–flying and reentering satellites (in–track location errors of several ki-

lometers can occur in periods of hours). The ionospheric current systems (known as "electro-jets") cause other observable effects, including the induction of electrical currents in large man-made conductors such as oil pipelines, telegraph or telephone lines, and power distribution grids.

The high-latitude ionosphere is strongly linked to the magnetosphere by the geomagnetic field, and the variations of the high-latitude ionosphere are mainly driven by geomagnetic activity whose origins lie within the magnetosphere. Figure 1 shows a noon-midnight meridian cross section[17] of the typical configuration of the geomagnetic field within the magnetosphere. The interaction of the solar wind, which flows at supersonic speeds (250 - 800 km/sec) relative to the earth, with the magnetosphere causes the formation of a bow shock at distances of ~ 10 earth diameters upstream in the solar wind. The region of hot compressed solar plasma between the bow shock and the boundary of the magnetosphere (the magnetopause) is known as the magne-tosheath. The "size" of the magnetosphere varies greatly, and is mainly determined by a balance between solar wind dynamic pressure and the magnetic pressure within the magnetosphere. The magnetospheric tail, which extends hundreds of earth diameters downstream (well beyond lunar orbit), results from tangential forces of the solar wind along the magnetopause. The mag-netotail is a poorly explored region of the magnetosphere, within which much of the mag-netospheric plasma energization is initiated. Generally speaking, the outer portions of the mag-netosphere are the most dynamic and are most strongly affected by variations in solar wind con-ditions. These outer regions magnetically "map" down into the ionosphere at very high lati-tudes. The inner radiation belts, which contain the most energetic and penetrating trapped radi-ation in the magnetosphere, do not respond significantly to the external solar wind effects. The inner portions of the magnetosphere map into the ionosphere at low latitudes, and these regions do not exhibit large responses to changes in geomagnetic activity.

The interaction of the solar wind with the magnetosphere is energetically quite efficient; it has been estimated that less than one percent of the incident solar-wind energy flux is ultimately dissipated within the magnetosphere[18]. The solar-wind energy couples into the magnetosphere more effectively when the interplanetary magnetic field (IMF) has a large component in a direc-tion opposite to that of the geomagnetic field. The solar wind-magnetosphere interaction sets up a large-scale convection pattern within the magnetosphere. Periods of "southward" IMF and high solar wind velocities are well correlated with enhancements of magnetospheric convection velocities. The magnetospheric plasma drifts in a circulation pattern from the dayside "cusp" region tailward over the polar caps, into the tail "lobes", through the plasma sheet where it be-comes nonadiabatically energized, then sunward again (being adiabatically energized as it en-counters higher magnetic field strengths nearer the earth) until the plasma finally exits the dayside magnetopause. The convection cycle is completed in about 12 - 20 hours. Periods of enhanced activity result in enhanced fluxes of hot plasma within the magnetosphere, and en-hanced rates of precipitation of plasma into the high-latitude ionosphere and atmosphere.

The plasma sheet which forms amidst this convection process contains hot plasma which can cause electrical charging of the surfaces of satellites, particularly those in geosynchronous
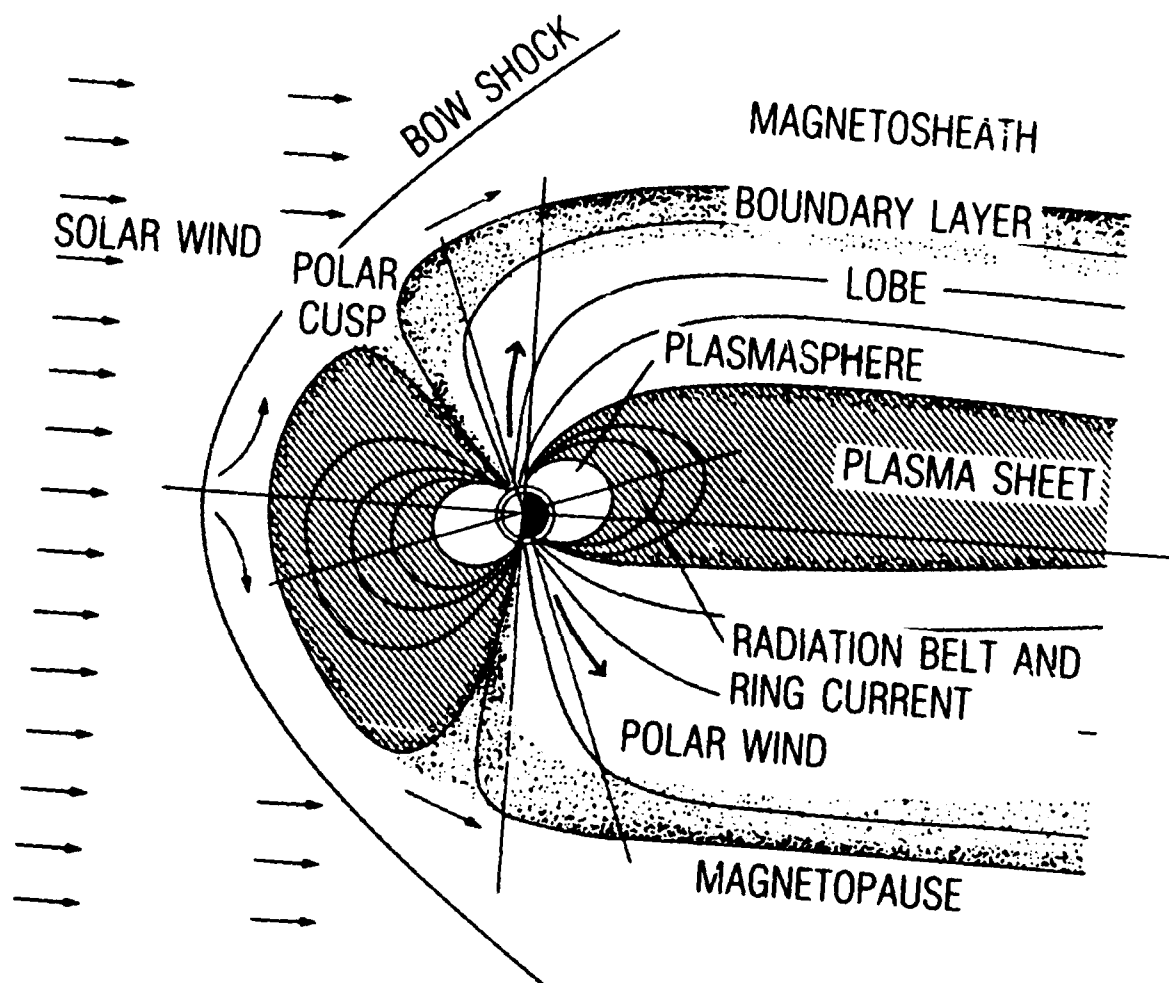
7

Figure 1. A Noon-Midnight Meridian Cross-Section View of Earth's Magnetosphere

8

orbits[19,20]. The earthward edge of the plasma sheet penetrates well inside of geosynchronous orbit during relatively high levels of geomagnetic activity. As plasma sheet particles drift earthward from the magnetotail, electrons tend to drift eastward (toward dawn), while ions drift westward (toward dusk). The most severe satellite surface charging events (and resulting electrostatic discharges) tend to occur in the midnight–to–dawn local time sector, where satellites encounter high fluxes of hot, drifting plasma–sheet electrons. The probability of occurrence and the severity of spacecraft charging events are directly correlated with periods of enhanced geomagnetic activity[20], corresponding to periods of enhanced convection and plasma sheet energization. Severe spacecraft charging events tend to occur during the equinox seasons, when geosynchronous satellites enter and exit earth eclipse once each day. In sunlight, photoelectron flux emitted from the satellite tends to balance current from the surrounding plasma. During eclipse, these vehicles cannot emit a photoelectron flux to balance the hot electron current from the plasma ($\sim 1 - 10 \, \mu A/m^2$), and electrical charging of the vehicles to several kilovolts is possible. Upon exiting eclipse, various surface materials discharge at different rates, creating the possibility of large differential potentials and discharges between external satellite components.

At altitudes below geosynchronous orbit, plasma motion is dominated by the effects of the earth's rotation. Low energy (thermal) electrons and ions execute more–or–less circular trajectories around the earth. The plasma trajectories are closed in the sense that the particles do not escape from the magnetosphere in steady–state conditions. The dominant source of low energy plasma in this corotating region is the ionosphere. The corotating region is known as the plasmasphere, and its outer boundary is called the plasmapause. Because the drift paths within the plasmasphere are closed and stable, relatively high plasma densities can develop there (equatorial densities of $100 - 1000 \, cm^{-3}$ can occur within the plasmasphere, compared with densities of $0.1 - 10 \, cm^{-3}$ in the outer magnetosphere). Although the plasmaspheric plasma does not have significant direct effects on spacecraft systems, the enhanced plasma densities do affect communications (for example, up to 10 percent of the total column electron content in a surface–to–geosynchronous radio propagation path can be due to plasmaspheric plasma). Also, the high plasma densities within the plasmasphere tend to modify the rates at which high–energy radiation belt particles are scattered into the ionosphere. Thus, the distribution of low energy plasma can affect other magnetospheric and ionospheric particle populations through secondary processes.

The radial position of the plasmapause is determined by the relative strengths of the electric fields associated with magnetospheric convection (variable) and the earth's rotation (constant). During geomagnetically quiet conditions the plasmasphere can extend outward beyond geosynchronous orbit. During disturbed conditions the outer portions of the plasmasphere are swept away by enhanced magnetospheric convection, and the plasmasphere might extend only one quarter of the distance to geosynchronous orbit. The erosion of the outer plasmasphere during geomagnetic disturbances can occur within an hour of the onset of enhanced convection, while the refilling of the plasmasphere can take days. Thus, the distribution of plasma tends to

be quite variable, and the shape of the plasmasphere depends both on the strength and on the time–history of geomagnetic activity.

During extended intervals of enhanced geomagnetic activity, large fluxes of trapped penetrating (> several hundred keV) electrons can develop within the outer electron zone and near geosynchronous altitudes. These penetrating electrons can become embedded within bulk dielectrics on satellites (e.g., cable insulation, printed circuit boards), building up electrical potentials over time which can exceed the breakdown potential of the dielectric[21]. Theoretical and experimental results[22,23] have shown that breakdowns occur when the integrated fluence of penetrating electrons exceeds about 10^{12} cm^{-2} in time periods shorter than the leakage time-scales of the dielectric (typically, several hours). These fluence levels are often exceeded in geosynchronous orbit over the several–day period following major geomagnetic storms. While the bulk–charging phenomenon can be eliminated through the use of modest shielding[21], external unshielded cables are used on many satellites nevertheless. Weak discharges resulting from bulk charging can cause spurious signals in the affected circuitry, while more severe discharges can damage some semiconductors. While surface charging events tend to be isolated to the region of drifting plasma sheet electrons in the midnight–dawn local time sector, bulk charging tends to occur at all local times because the penetrating electrons tend to be distributed more uniformly and because the phenomenon is a cumulative effect.

Obviously, the effects of solar activity on near–earth plasmas and, in turn, on man–made systems are quite varied in magnitude, timescale, and predictability. It is reasonable to classify the effects into two categories: (1) direct, abrupt effects, usually caused by rapid changes in solar UV and x–ray illumination of the earth's atmosphere and ionosphere during the occurrence of solar flares, and (2) indirect effects which are caused by more complex interactions between solar particles and the solar wind on the coupled magnetosphere–ionosphere system. The direct effects can be understood more easily, but they are not necessarily any more predictable. Certainly the frequency of occurrence (though not necessarily the severity) of optical and X–ray flares and solar proton events correlates well with the 11–year sunspot cycle[6], and an extreme solar maximum would almost certainly involve more major flare occurrences. Typically the magnitude of the "background" solar UV flux tracks the sunspot number fairly well, even though the total visible radiation from the sun can be diminished slightly (~ 1%) during occurrences of large (dark) sunspot groups. The relationship between the solar cycle and the physical parameters of the solar wind which (indirectly) cause geomagnetic disturbances at the earth is more complicated and requires a closer look.

Figure 2 shows a schematic drawing of the relationship between large–scale structures in the interplanetary magnetic field and the earth in its orbit around the sun[24]. As the solar wind expands outward from the sun, it tends to retain the large–scale inhomogeneities which were present in the solar corona. The majority of the solar wind plasma flows outward along open magnetic field lines connected to coronal holes[25]. Coronal holes are relatively cool regions of the corona which generally occupy the polar regions of the sun, but can extend to solar equatorial latitudes, especially during the declining phase of the solar cycle[26]. Typically, active regions

THE SOLAR CURRENT SHEET

EARTH ORBIT
ABOVE ——
BELOW ----
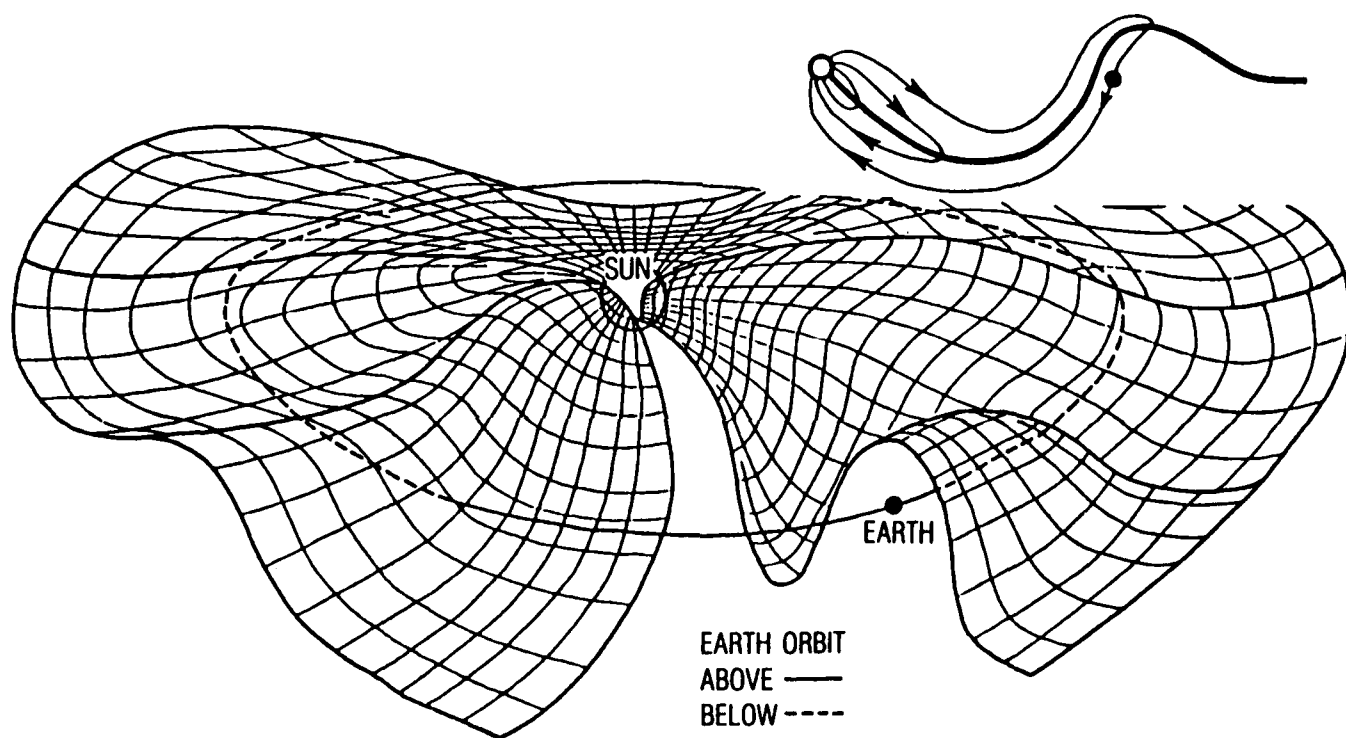
Figure 2. A Schematic Representation of the Relationship Between the
Earth's Orbit and the Warped Solar Current Sheet

on the sun have a magnetic field topology which is closed and dipole-like. Solar wind outflow in coronal holes draws the solar magnetic field lines outward away from the sun in a configuration similar to that of the earth's magnetotail. A current sheet (again similar to that which forms in the earth's magnetotail), shown graphically in Figure 2, separates magnetic fields whose polarity is either "toward" or "away from" the sun. Large-scale structure in the corona and solar wind produces the notable "warping" of the solar current sheet[27]. The insert in the upper right portion of Figure 2 depicts the relationship between the position of the earth relative to the solar current sheet and the magnetic field orientation. It is obvious that an observer on the earth experiences a magnetic field orientation which is very much affected by coronal inhomogeneities and by the position of the earth relative to the solar current sheet. Temporal variations in the observed solar wind velocity and magnetic field orientation and magnitude are caused by the coupled effects of the solar wind outflow and the solar rotation, along with other magnetohydrodynamic processes within the solar wind such as shock formation, turbulence, waves, discontinuities, and magnetic field compressions due to large coronal mass ejections[28].

Aside from the interplanetary magnetic-field configuration depicted in Figure 2, the most important solar wind features for solar-terrestrial effects are solar wind streams. Figure 3 depicts the basic characteristics of a solar wind stream[24], shown as a cross section in the solar-ecliptic plane. The solar wind flows radially outward from the rotating sun, carrying with it the "frozen in" coronal magnetic field into a resulting spiral pattern. A region of high-speed flow (the shaded region in Figure 3), which might result from the equatorward protrusion of a coronal hole, also flows outward in a spiral pattern but its spiral is coiled less tightly than that of the slower-moving surrounding plasma. The high-speed stream thus flows outward through the slower plasma, resulting in compression of the plasma and the possibility of shock formation at distances near the earth's orbit.

A great deal of observational evidence supports the hypothesis that the solar wind speed has a dominating influence on geomagnetic activity and related phenomena. Figure 4 shows stacked plots of six-month averages of the solar wind speed and of the global geomagnetic activity index ap[29,30]. [The solar wind data are from the Mariner 2 data set (1962) and from the Vela and Imp spacecraft (1964–1975).] The ap index is a planetary magnetic activity index which has a roughly linear relationship to the magnitude of observed global geomagnetic deviations. The correspondence between the two plotted quantities is clear. For long-term averages (~ months) the ap index is found to correlate best with the *square* of the solar wind velocity, with a correlation coefficient greater than 0.8. (The correlation is so good that many researchers of historical solar data have been tempted to use geomagnetic activity indices as proxy data for solar activity measurements.)[31-34] On shorter time scales, which are more representative of the geomagnetic events themselves (~ minutes to hours), the correlation between solar wind speed and geomagnetic activity is much poorer. For these shorter time scales[35,36], the magnitude and direction of the interplanetary magnetic field (IMF) appears to have a controlling influence on the level of geomagnetic activity. Specifically, the occurrence of sustained intervals of an IMF with a significant southward component is well correlated with the onset of geomagnetic storms. However,
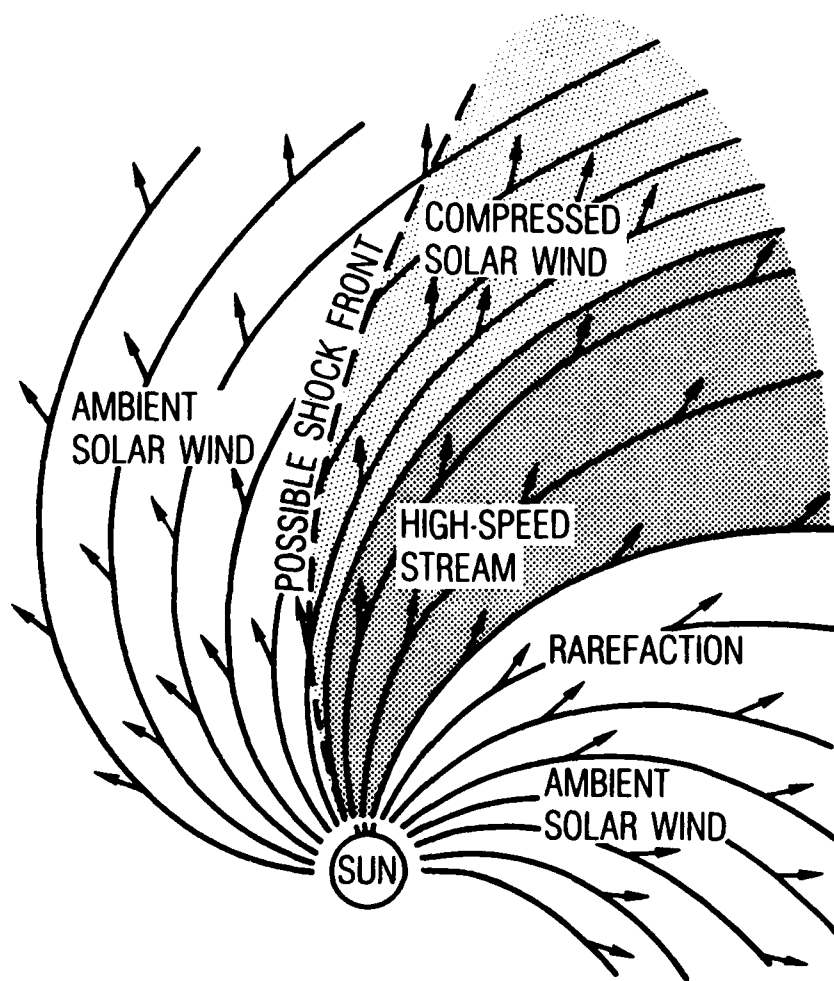
Figure 3. A Solar-Ecliptic Cross Section of the Interaction of a High-
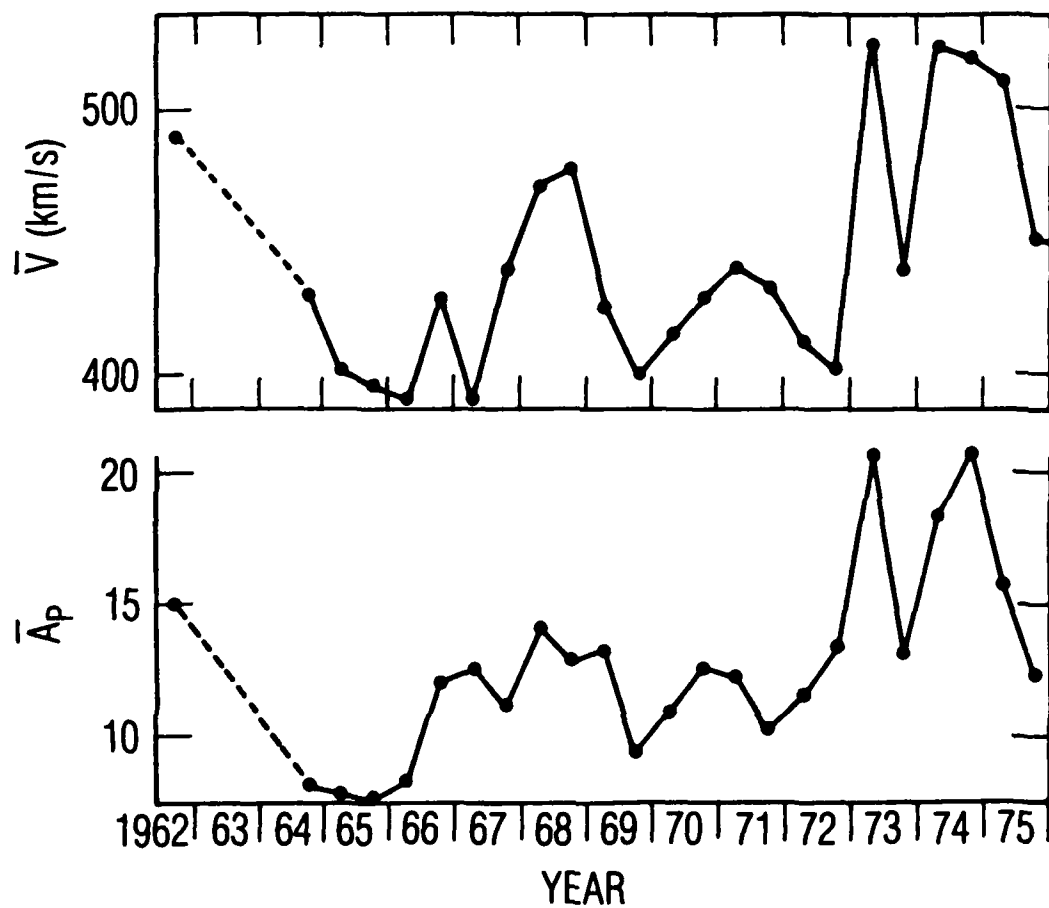Speed Solar Wind Stream with the Ambient Solar Wind

13

Figure 4. Six–Month Averages of the Solar Wind Speed and the Geo-
magnetic Activity Index AP

14

the IMF is very poorly correlated with geomagnetic activity over long time scales (the correlation coefficient between six–month averages of the IMF Bz component and the ap index is less than 0.03)[30]. It appears as though the overall envelope of geomagnetic activity is well correlated with the solar wind speed, while individual events may be "triggered" or at least modulated by the IMF. Other solar wind parameters, such as the plasma density and temporal variances of the speed and the IMF, have been found to correlate weakly with the level of geomagnetic activity as well. Table 1 summarizes a group of published empirical and theoretical relationships between solar wind parameters and various measures of geomagnetic activity[30,37-44].

Functional relationships between solar wind and geomagnetic parameters provide important information on the processes which couple energy between the two systems. The relationships are also useful for scaling the effects of anticipated enhancements in solar activity in terms of geophysical effects. However, for practical purposes it would be more useful to be able to predict the expected number and severity of individual geomagnetic "events" than to have a clear understanding of how average quantities might vary from year to year. As is the case for many interactions between man and nature, the occasional occurrence of extreme conditions (hurricanes, tornados, volcanic eruptions, earthquakes, etc.) can be more critical than longer–term variations. Certainly this is the case for modern space systems. Unfortunately, the complexity of solar–terrestrial interactions makes it difficult to predict events or even to compile usable statistical information on geomagnetic events.

Table 1. Empirical and Theoretical Relationships Between Geomagnetic
Activity and Solar Wind Parameters

Source Reference	Geomagnetic Activity Index	Functional Relationship to Solar Wind Parameter(s)
Snyder et al.[37]	ΣK_p	$\Sigma K_p = (V-330)/8.44$
Olbert[38]	ΣK_p	$\Sigma K_p = (V-262)/6.30$
Garrett et al.[39]	ap,AE	$ap,AE = C_1 + C_2 V B_z + C_3 V^2$
Murayama and Hakamada[40]	AE	$AE = C B_z V^2$
Burton et al.[44]	Dst	$\delta Dst/\delta t = F(V B_z) - C_1 Dst$
Crooker et al.[30]	ap	$ap = 3.5 \times 10^{-5} B_z V^2 - 1.9$
	ap	$ap = 7.0 \times 10^{-5} V^2 - 1.8$
Feynman and Crooker[43]	aa	$aa = 1.3 + 4.7 \times 10^{-5} B_z V^2$
Maezawa[41]	AL	$AL \sim B^{0.85} V^{2.08} (\sin \Theta)^{0.54}$
	AU	$AU \sim B^{0.67} V^{1.15} (\sin \Theta)^{0.34}$
	am	$am \sim B^{1.03} V^{2.34} (\sin \Theta)^{0.37} n^{0.2}$
Murayama[42]	AL	$AL = 60 (B_z + 0.5) V^2 n^{0.13} F(B_y)$

A major part of the problem of studying geomagnetic activity in terms of "events" is depicted in Figure 5, which shows several hypothetical representations of the coupling of energy between the solar wind and the terrestrial system[11]. If the interaction were a purely driven process, the solar wind energy (ϵ) would couple directly into the magnetosphere and be dissipated (U_T), perhaps with some characteristic time delay (τ). The time series of energy dissipation (a combination of particle energization, joule heating of the atmosphere, auroral activity, and other processes which affect man–made systems) would be well correlated with the solar forcing, and the terrestrial effects would be easy to predict. In an unloading or triggered process, the solar wind energy first would be be stored, then released at some later time, possibly by an independent triggering mechanism. In an unloading system, the onset, magnitude, and duration of a geomagnetic "event" need not be well correlated with the forcing. Event prediction would require complete knowledge of the energy coupling process, the storage mechanism, and the triggering mechanism. In reality, the terrestrial system exhibits characteristics of both a driven and a triggered system. Even worse, some individual events exhibit a mostly driven character, while others respond as an unloading system. Thus, it is difficult to predict which solar events will cause the most extreme geomagnetic conditions. Also, this complex coupling behavior can lead to difficulty in interpreting statistical parameter correlations. In particular, some parameters which correlate on short time scales may not correlate well for long term averages, and parameters which correlate in a long term average may not be good predictors of individual events. We have seen some evidence of this effect in the statistical correlations between solar wind velocity or the IMF with geomagnetic activity, and in the variety and occasional disparity between the parametric relationships listed in Table 1. It is important to recognize that the formulations listed in Table 1 apply only on time scales characteristic of the averaging period for the individual activity indices, and that none of the formulations offer a true predictive capability for extreme events.
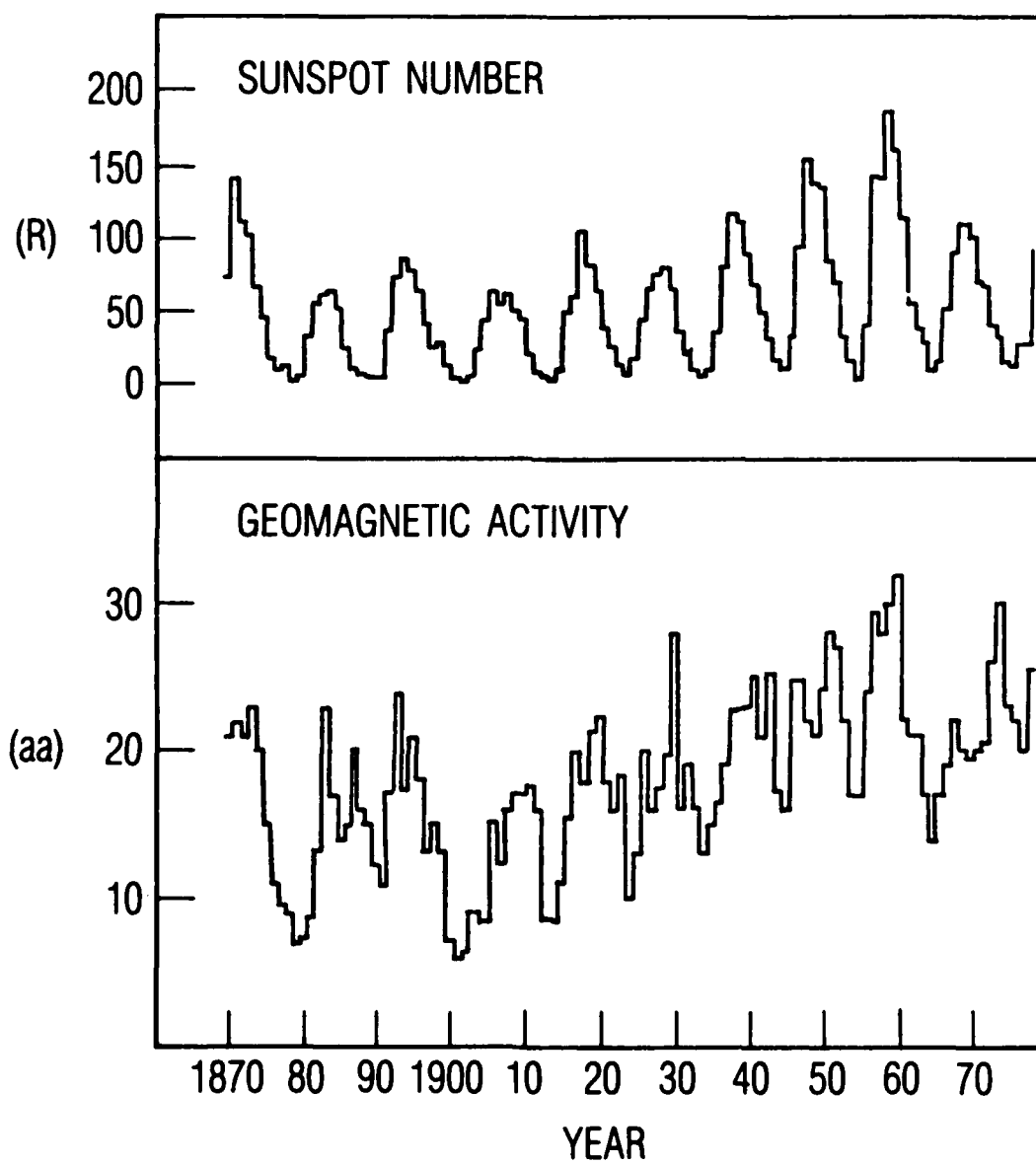
Figure 5. Examples of Energy Coupling in a Purely Driven System, a
Purely Triggered System, and a Complex System

3. THE RELATIONSHIP BETWEEN THE SUNSPOT CYCLE AND GEOMAGNETIC ACTIVITY

The preceding section summarized the major interactions between solar activity and the near–earth plasma environment. Several processes which effectively couple solar electromagnetic or particulate energy into the magnetosphere/ionosphere/atmosphere system were identified, and numerous potential effects on man–made communications and space systems were cited. A number of parametric relationships between solar and geophysical parameters were identified, and the importance individual geomagnetic "events" was established. The purpose of this section is to assess how those solar parameters which most directly affect the terrestrial plasma environment vary during a sunspot cycle and to examine the relationship between the magnitude of the sunspot maximum and the occurrence and magnitude of geomagnetic events.

While sunspots themselves have virtually no effect on geomagnetic activity, other solar parameters which do affect the terrestrial environment (e.g., flares, coronal holes, solar wind streams, etc.) tend to be modulated along with sunspot numbers in an 11–year cycle. Also, the modulation amplitude of many solar parameters tracks the sunspot number fairly closely[45]. Thus, we might expect geomagnetic activity to be modulated at the 11–year sunspot cycle period by acquaintance[39,46]. Figure 6 shows this to be the case. Figure 6 plots yearly averages of the sunspot number and an index of geomagnetic activity[47] from 1869 to 1975, including data from solar cycles 11 to 21. The geomagnetic activity index shows a clear modulation corresponding to the 11–year sunspot cycle. However, the annual averages of geomagnetic activity do not maximize at the time of sunspot maximum, nor do the cyclic peaks of geomagnetic activity correspond in amplitude to the amplitude of the nearest sunspot maximum. On closer inspection, the geomagnetic index tends to have a double–peaked modulation, with the major peak occurring during the declining phase[48] of the sunspot cycle and a secondary peak occurring nearer to the sunspot maximum[49,50]. The major peak is probably due to the tendency for strong recurrent solar wind streams to occur primarily during the sunspot declining phase. Both sunspots and coronal hole regions tend to occur at progressively lower solar latitudes as the sunspot cycle proceeds. Equatorial protrusions of coronal holes are a major source of strong recurrent solar wind streams, which are known to cause geomagnetic activity[51,52].

The geomagnetic activity shows some evidence of a trend toward increasing magnitudes over the past several solar cycles[47,53]. The trend is especially apparent in the cyclic minimum values of the geomagnetic activity index. This feature has prompted some researchers to hypothesize a long–period (~ 80–year) cyclic behavior of solar wind parameters[54]. If this long–period modulation persists into the next solar cycle we might expect somewhat higher average levels of geomagnetic activity even for typical values of sunspot numbers. As yet no firm physical basis has been identified for the longer–period behavior, and it would be risky to use the observed trend for predictive purposes.

In light of the several recent predictions of enhanced sunspot activity for the upcoming solar cycle 22, it would be useful to have some feeling for the overall relationship between the ampli-
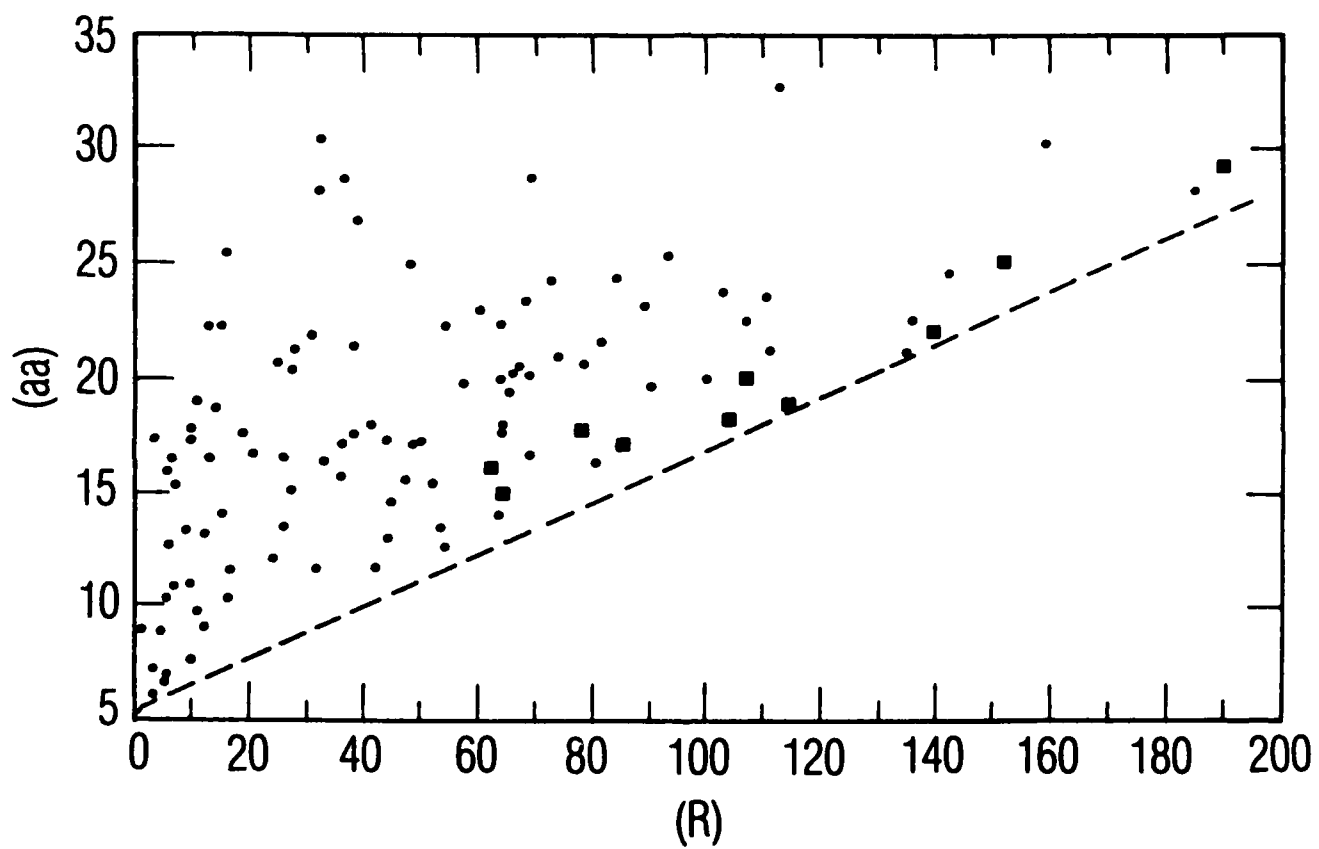
Figure 6. Annual Averages of Sunspot Number and Geomagnetic Activity from 1869 to 1975

tude of the solar cycle and the magnitude of geomagnetic activity (if any relationship exists). Does a large sunspot number really mean enhanced geomagnetic activity? A relationship, of sorts, does exist. Figure 7 plots annual averages of geomagnetic activity versus annual sunspot numbers[47] from the same data set shown in Figure 6. While the linear correlation between the two parameters is relatively poor, a clear relationship between the parameters is apparent nevertheless. Specifically, larger values of sunspot numbers seem to exclude the possibility of occurrence of low levels of geomagnetic activity. However, the highest values of geomagnetic activity do not necessarily occur during the years of highest sunspot numbers. The equation which represents the minimum activity for a given value of sunspot number is[47]

$$aa_{(ave)} = 0.12 \, R + 5.38 \tag{1}$$

An interesting aspect of this relationship is that *if* the upcoming solar maximum is historically extreme (i.e., sunspot numbers in excess of 200 or so) then the average level of geomagnetic activity almost certainly will be historically extreme as well.

Data points corresponding to the individual years of solar cycle maxima are plotted with heavier points in Figure 7. A curious feature of these particular data points is that they all lie very near the line of *minimum* geomagnetic activity. The implication is that solar activity is less effective in coupling to the terrestrial system during the solar maximum years than during the declining phase of the solar cycle. Again, this behavior is due to the tendency for strong recurrent solar wind streams to be spawned by low–latitude coronal holes late in the solar cycle. If this relationship holds for solar cycle 22, the actual occurrence of an extreme solar maximum in 1990 or 1991 may be an excellent predictor of enhanced geomagnetic activity during the subsequent declining phase of the solar cycle.

In the preceding section of this report, statistical results were presented which demonstrated a strong correlation between solar wind speed and geomagnetic activity. This relationship offers a reasonable explanation for many features of the correlation and phasing of the sunspot and geomagnetic activity cycles shown in Figure 6. Figure 8 shows histograms of the occurrence frequency distributions of solar wind speed over a period spanning a complete solar cycle[29]. The histograms are plotted yearly, from 1962 to 1974. The arrow on each plot shows the average speed for each year. Note that the average solar wind speeds are slightly enhanced in the solar maximum year 1968 and in the declining phase years 1962, 1973, and 1974. More importantly, note that the occurrence of extreme solar wind streams (speeds in excess of 700 km/sec) occur much more often in the declining phase years than in other phases of the solar cycle. The occurrences of these extreme values of solar wind speed are best correlated with the highest levels of geomagnetic activity for this time period.

The interplanetary magnetic field also plays a significant role in coupling solar wind energy to the magnetosphere. Figure 9 shows monthly averages of sunspot number, the geomagnetic activity index aa, and the critical component of the IMF (negative values of B_z correspond to the
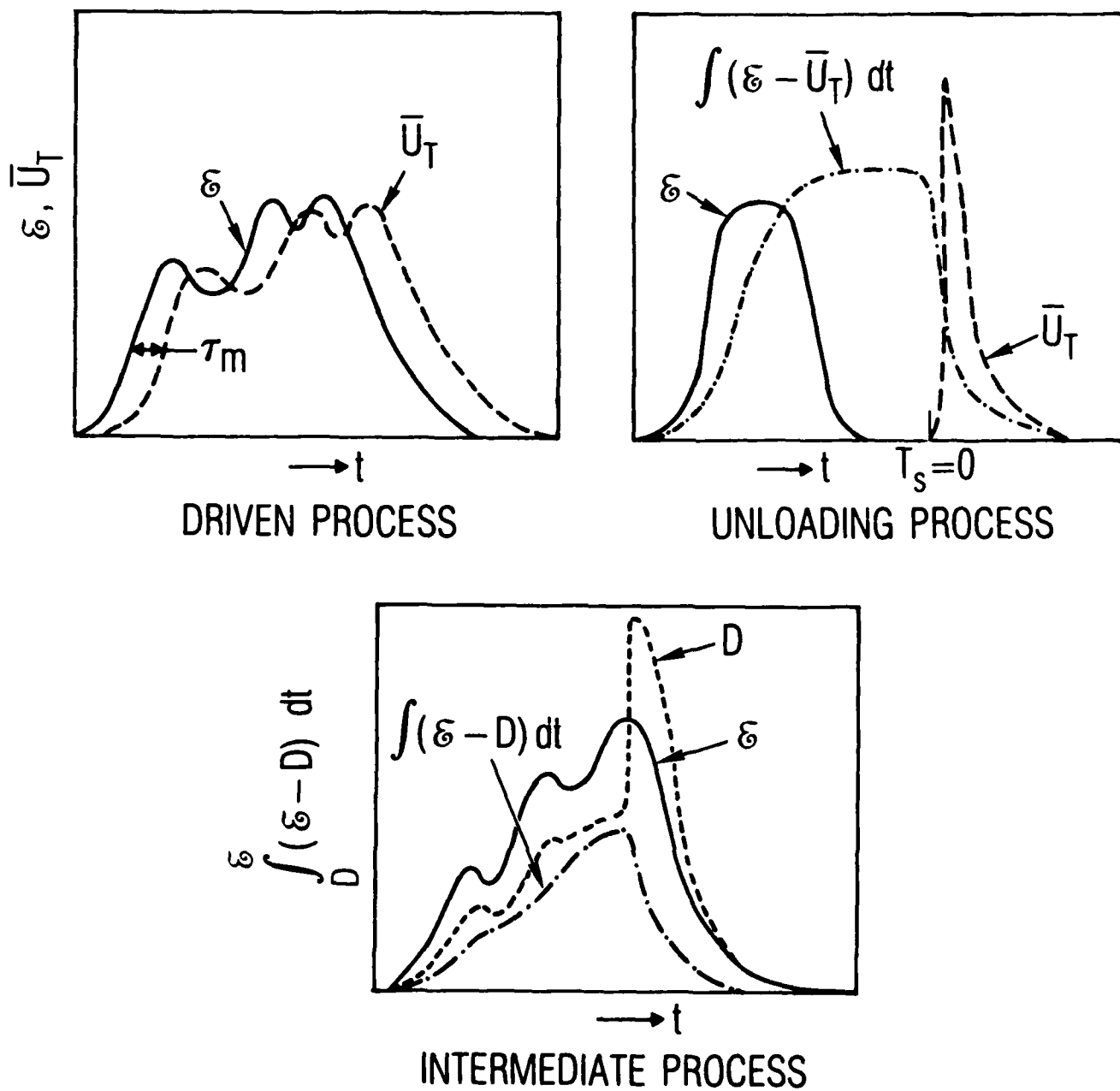
Figure 7. Annual Averages of Geomagnetic Activity vs Sunspot Number for the Same Data Plotted in Figure 6
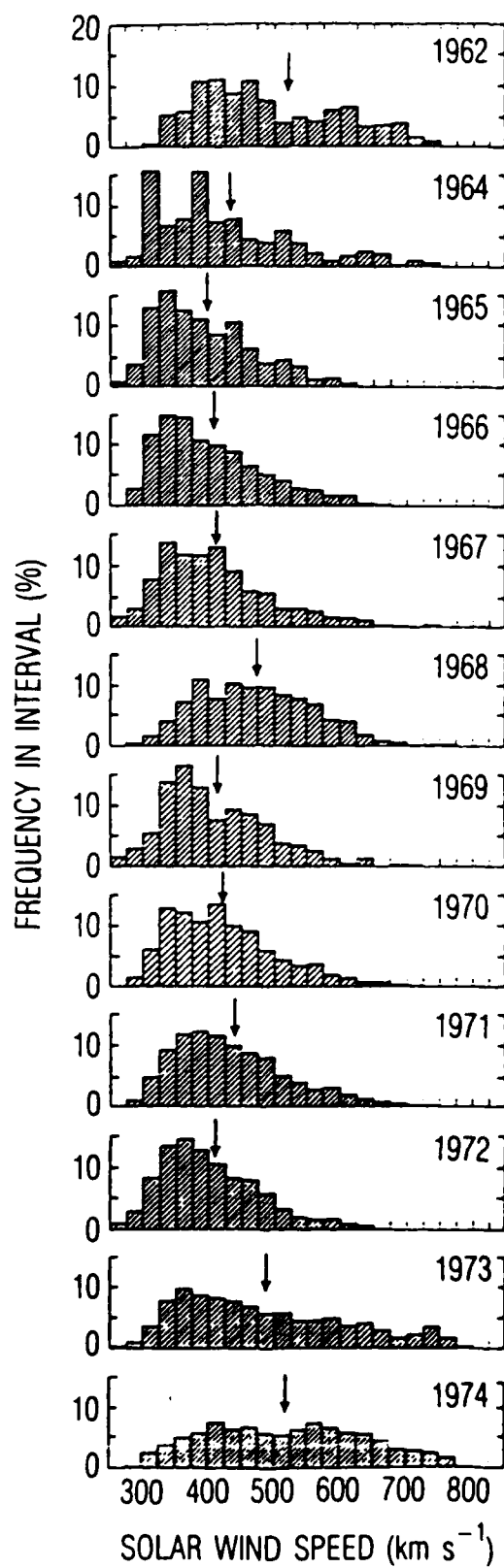
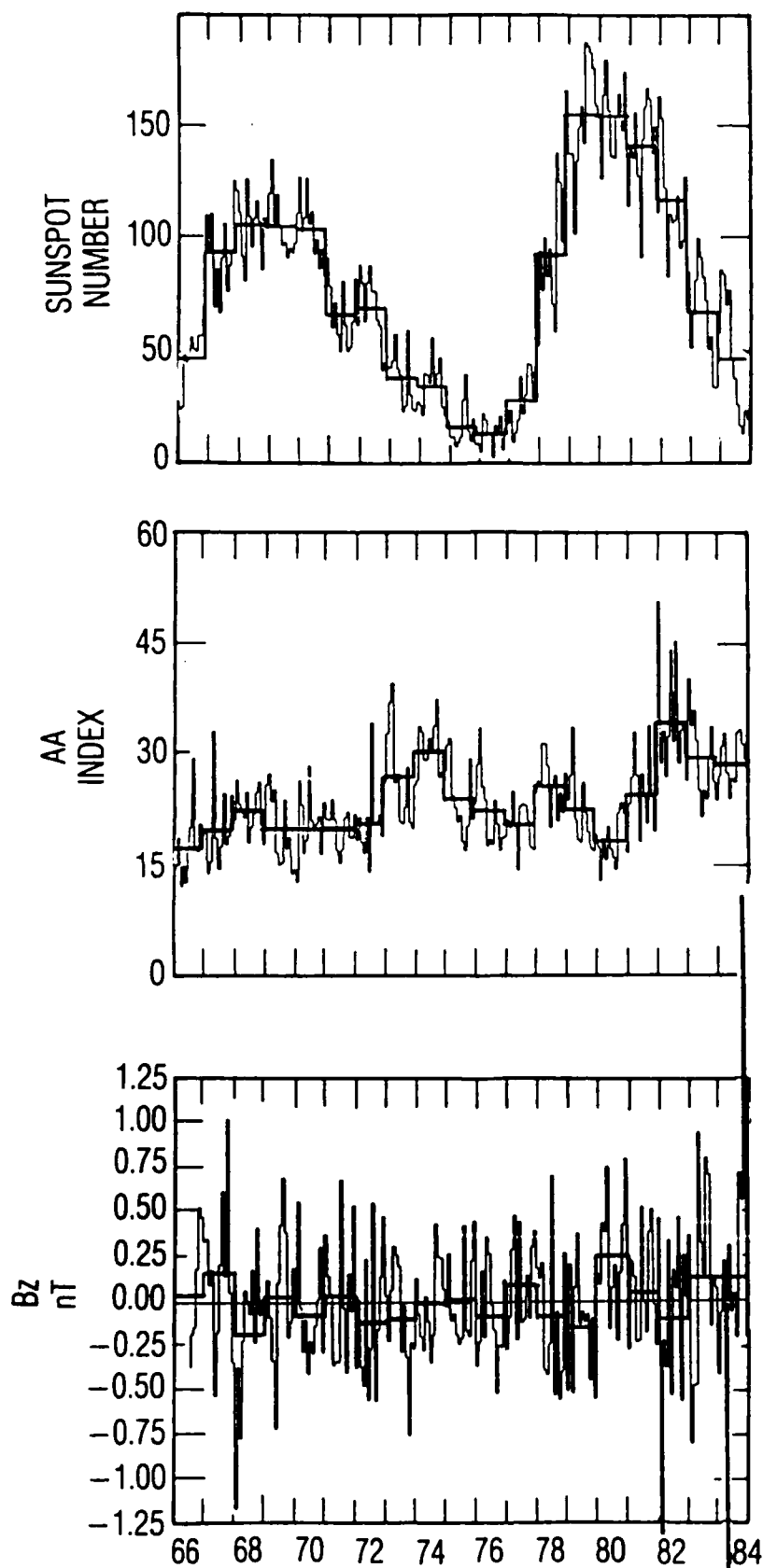**Figure 8.** Histograms of Solar Wind Distributions for the Years 1962–1974

Figure 9: Monthly Averages of Sunspot Number, Geomagnetic Activity, and the Interplanetary Magnetic Field Z–Component for Solar Cycles 20 And 21.

"preferred" southward fields) for solar cycles 20 and 21.[55] Peaks of geomagnetic activity in the declining phase years (1973–1975 and 1981–1983) are evident. The plot of IMF B_z shows no significant trend or correlation with the solar cycle or with the cycle of geomagnetic activity. The monthly average values of IMF B_z tend to be small (< 1 nT) compared to the average total magnitude of the IMF (~ 5 nT). Other studies have shown 10–15% variations in IMF intensity in phase with the sunspot cycle and a slight tendency for large IMF values (> 10nT) to occur more frequently within a few years of sunspot maximum[56], but no clear IMF modulation has been identified. The implication of this result is that the IMF B_z component does not manifest a controlling influence over the occurrence or magnitude of geomagnetic activity on time scales comparable to the solar cycle, but that short–term occurrences of southward IMF are distributed throughout the solar cycle and act in concert with solar wind streams to produce geomagnetic events. While the IMF may be an important parameter in the physical coupling between the solar wind and magnetosphere on short time scales, it does not appear to carry any long–term predictive qualities which could be projected into the upcoming cycle.

The observed correlations between solar activity and geomagnetic activity imply that many communications and space systems could be adversely affected during an extreme solar maximum and for several years thereafter. It should be noted that the cited correlations have utilized very crude indices of geomagnetic activity. Measurements of the solar cycle dependences of the actual plasma parameters (i.e., plasma temperature, density, composition) which cause adverse effects, such as spacecraft charging, are rare and difficult to accomplish[57,58]. This difficulty arises from the finite lifetimes of experimental satellites (typically much less than 10 years) and from uncertainties in cross–calibration of instruments on different satellites. In the case of magnetospheric plasmas, a crude measure of geomagnetic activity may be the most practical indicator of the expected environmental effects.

Somewhat more comprehensive data and more rigorous theoretical treatments are available for ionospheric effects. Typically, solar–illumination effects on the ionosphere tend to be direct effects which are relatively easy to quantify. For example, ionospheric critical frequencies are known to respond to variations in solar activity with the following (approximate) dependence[59]:

$$f_oF_1 \text{ (MHz)} = (4.3 + 0.01 \text{ R}) (\cos \chi)^b \qquad (2)$$

where χ is the solar zenith angle and b ~ 0.5. The linear dependence on sunspot number implies important consequences of an enhanced (e.g., R ~ 200) solar maximum. Indeed, the effects of enhanced solar UV and EUV radiation on the ionosphere could be the most global and most prolonged of all of the effects of the solar cycle on the terrestrial system.

The ionospheric effects on communication links have been studied for extended periods of time with a large variety of measurement techniques. Some of the most effective measurement techniques are the communications systems themselves, from which qualitative but useful data on ionospheric "weather" conditions can be acquired globally. Indeed, skilled shortwave radio operators can sense, analyze, correct for, and even utilize changing ionospheric conditions in

near-real time. More quantitative ionospheric sensing over the past several decades has included riometry, backscatter radar, ionosondes, *in situ* measurements from rockets and satellites, topside ionospheric sounders, multiwavelength ionospheric imagery, and ground-satellite radio beacon measurements. Each of these sensing techniques has contributed immense data sets over the years on both the large-scale and small-scale ionospheric responses to changing solar and geomagnetic conditions. Much of these data and related theoretical formulations have been incorporated in numerical (parameterized) ionospheric specification models for operational applications[45]. Some specific examples of parameterized relationships between solar or geomagnetic activity indices and ionospheric parameters are listed in Table 2. Note the relatively independent nature of the global (mid-latitude) and auroral (high latitude) ionospheric effects.

Table 2. Empirical Relationships Between Solar-Geomagnetic Activity
Indices and Ionospheric Parameters[60]

Source Reference	Ionospheric Parameter (units)	Functional Relationship	
Davies[59]	f_0F_1 (MHz)	$f_0F_1 = (4.3 + 0.01R)(\cos \chi)^b$	
		$b = 0.2 + 0.3(\chi-90)/15.5$	
Lloyd et al.[61]	hmF_1 (km)	$hmF_1 = 165 + 0.642\chi$	
Elkins and Rush[62]	f_0E_{solar} (MHz)	$f_0E_s = A(\cos \chi)^m[(1-.0038(12-T)-.00013ap)]$	
		$m = 0.25$	
Elkins and Rush[62]	hmE (km)	$hmE = 100 + 20 \ln(90\chi_E)$	
		$\chi_E = \chi (90/101)$	$(\chi < 76.78°)$
Wakai[63]		$hmE = 120$	$(\chi > 76.78°)$
Gassman[64] and Vondrak et al.[65]	$f_0E_{auroral}$ (MHz)	$f_0E_a = 2.5 + Q_E/9$	$0 < Q_E < 2.7$
		$f_0E_a = -1.0 + 7Q_E/5$	$2.7 < Q_E < 4.2$
		$f_0E_a = 3.2 + 2Q_E/5$	$Q_E > 4.2$
Gassman[64] and Vondrak et al.[65]	hmE_a (km)	$hmE_a = 185$	$f_0E_a < 2$
		$hmE_a = 185-30(f_0E_a-2)$	$2 < f_0E_a < 3.5$
		$hmE_a = 145-10(f_0E_a-3)$	$3.5 < f_0E_a < 9$
Wagner[66]	f_0E (km)	$f_0E = [1.5(f_0E_a)^4 + (f_0E_s)^4]^{1/4}$	

In addition to the direct variations of ionospheric parameters caused by solar or geomagnetic activity, the formation of small–scale ionization irregularities can cause severe impacts on VHF/UHF communications links[13]. Time–varying small–scale (< 1 km) irregularities can cause amplitude and phase scintillation of transionospheric radio links and tracking radar signals at VHF through UHF frequencies. The effects of ionization irregularities on transionospheric radio links has been studied directly over the past several years through the use of space–based radio beacons in low polar orbit, in geostationary orbit, and on the Global Positioning System (GPS) satellites. By positioning ground–based receivers at several sites worldwide, and by operating the receivers continuously over several years, comprehensive data on the effects of solar and geomagnetic activity on the formation of ionospheric irregularities and on the occurrence of signal fades have been acquired. Figure 10 shows an example of a long–term data set acquired from a VHF (250 MHz) receiver at Thule, Greenland[13]. The plot shows the monthly–average occurrence frequency of signal fades at four different levels (> 5 dB, > 10 dB, > 15 dB, and > 20 dB) over the 1979–1986 time period, spanning the solar–cycle 21 maximum and subsequent minimum. A clear correlation between the frequency and severity of signal fades with sunspot number is evident. Note that severe (> 20 dB) signal fades can occur as much as 50% of the time during solar maximum (weak fades occur as much as 90% of the time), while even weak (5 dB) fades occur less than 5% of the time during solar minimum years. At high latitudes, seasonal modulation is as important as any other factor in determining fade occurrence frequency. Kilometer scale irregularities do not tend to occur during the local summer solstice at high latitudes. Figure 10 shows that extreme solar activity levels certainly would be accompanied by high frequencies of severe VHF fades at high latitudes. On the other hand, signal fades (at VHF and UHF) are a relatively common and important problem even during modest solar activity.

Figure 11 summarizes the global occurrence characteristics of L–band fades for both solar maximum and minimum periods[13] (with some extrapolation of VHF results). Three regions of ionospheric scintillation are identified: the equatorial region in the post–sunset local time period, the auroral band, and the polar cap region. The most disturbed areas occur on either side of the equator. Scintillation effects maximize where the local magnetic dip angle is about 30°, with more moderate levels of scintillation occurring directly over the equator. Scintillation activity at higher latitudes tends to be more moderate than that near the equator. Greater temporal variability at high latitudes leads to different rms phase deviations and decorrelation times than for the same "intensity" of scintillation at lower latitudes. At solar minimum, scintillation activity in all three regions and at all frequencies is greatly reduced. Near the equator, 5 dB fades at L band are fairly uncommon. The most severe region tends to be the polar cap, where 5 dB fades can occur in patchy regions about 10% of the time. During solar minimum, rms phase deviations (at 250 MHz) rarely exceed 1 rad. For each of the plots shown in Figure 11, it should be noted that the scintillation levels at high latitudes are well correlated with occurrences of geomagnetic activity, while the lower–latitude scintillation occurrences are not well correlated with geomagnetic activity.
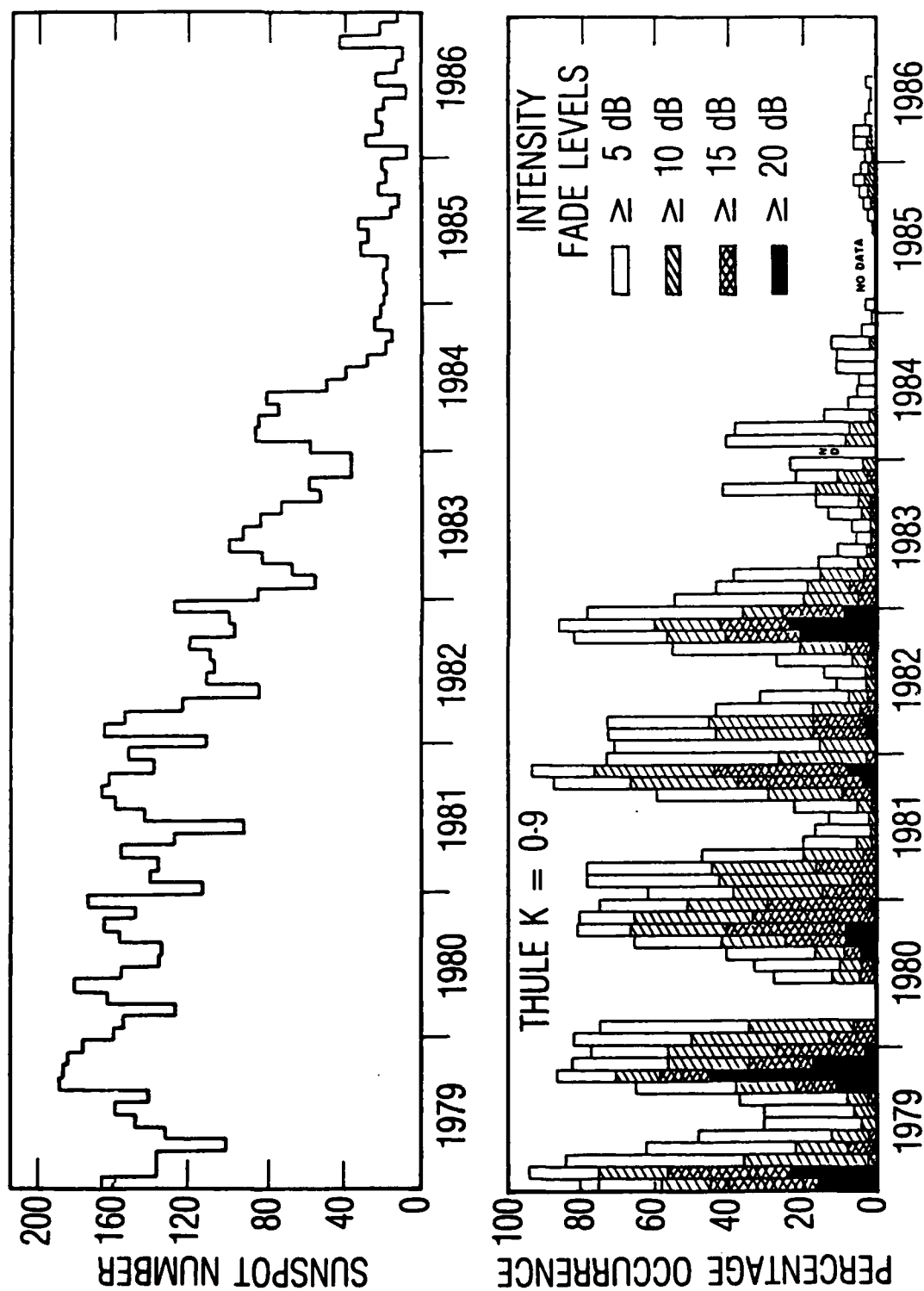
Figure 10: Histograms of the Occurrence Frequency of Signal Fades at Thule, Greenland, Compared to Monthly-Average Sunspot Number from 1979 to 1986.
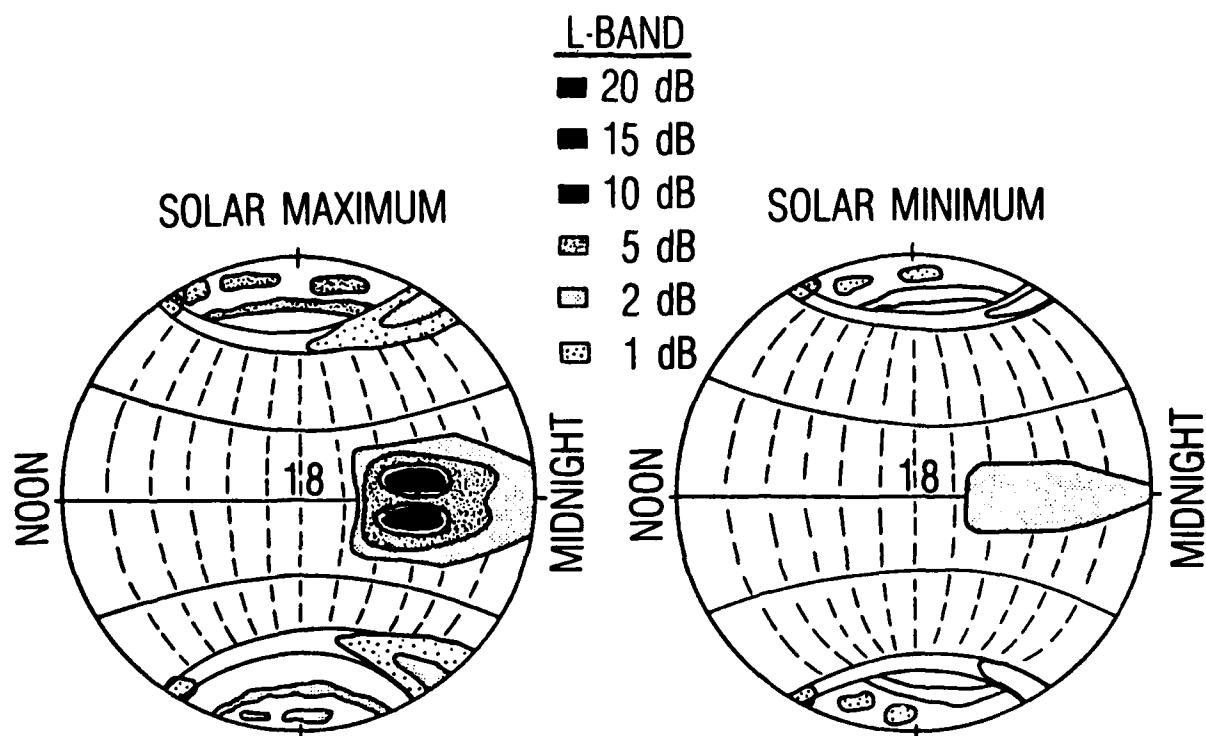
28

Figure 11. Local–Time–Latitude Plots of the Regions and Severity of
Signal Fades During Solar Maximum and Minimum Periods

4. SUMMARY

The observed rate of increase in solar activity at the initiation of solar cycle 22 has lead to the anticipation that the activity during the solar maximum years, 1990–1991, may be the most severe of any period during the space age. Solar activity has many effects on man–made systems in space, on ground or aircraft communications, and on communications systems that penetrate the ionosphere. The effects of solar activity include prompt, direct effects which result from enhanced levels of solar UV and X radiation, and the indirect effects of enhanced geomagnetic activity caused by the interaction between the solar wind and the terrestrial magnetosphere–ionosphere–atmosphere system. Aside from occasional solar radio noise bursts, solar activity itself does not cause substantial effects or interference with man–made systems. More typically, enhanced solar activity causes changes in the terrestrial environment. Interactions between man–made systems and the disturbed local environment account for the majority of solar effects on these systems. The most prominent effects on space–based systems include electrostatic discharges which result from the interaction between satellites and the magnetospheric plasma and penetrating radiation environment, single event phenomena which result from solar or galactic cosmic ray impacts within microelectronic devices, and communication or tracking problems related to ionospheric disturbances.

Disturbances in the near–earth plasma environment are closely tied to solar wind characteristics. Statistical data, case studies, and theoretical results indicate that the solar wind speed is the most important factor affecting geomagnetic activity over long time scales. This is an important result because the occurrence of high–speed solar wind streams is well correlated with other measurable characteristics of solar activity, such as sunspots. The interplanetary magnetic field, which does not have a strong correlation with the solar cycle, has been shown to correlate well with geomagnetic disturbances on short time scales. Many empirical and theoretical relationships exist which provide quantitative measures of the influence of these solar wind parameters on geomagnetic activity levels, but few of the results offer a true predictive capability for the upcoming cycle.

For practical purposes, such as estimating the effects of solar activity on operational space systems (for example, estimating the expected incidence of severe surface or bulk charging events) or on communications systems (for example, estimating the expected occurrences of severe "fades"), a method for predicting severe individual geomagnetic "events" may be more useful than relationships which correlate time–averaged geophysical parameters. This is the case for other interactions between man and his environment as well. Although it may be useful to know whether it is going to be slightly warmer or colder tomorrow, it is more important to know if there is going to be a thunderstorm, and much more important to know if a hurricane or tornado is expected. It is one thing to know that you live near an active seismic fault, but quite another to know when the "big one" is going to happen and how big it will be. Unfortunately, solar–terrestrial physics (along with meteorology and seismology) is at a very early stage in offering predictive capability for "events". However, it is safe to say that *if* solar cycle 22 is historically

extreme, *then* geomagnetic activity and its related effects also will exhibit historical levels during, and for a few years after, the solar maximum years.

REFERENCES

1. Schwabe, M., *Astronomische Nachr.*, Vol. 21 (1849, p. 234).

2. Schwabe, M., *Bern Mitt* (1851, p. 41).

3. Wolf, A. R., *Astr. Mitt. Eidg. Stern.*, Vol. 10 (1858, p. 6).

4. Galilei, G., "Letters on Sunspots, 1612," in *Discoveries and Opinions of Galileo*, Doubleday and Company, Inc., New York, 1957, pp. 106–119.

5. Maggs, W., W., "Biggest Solar Maximum Coming?," EOS, Vol. 69 (July 1988, p. 697).

6. Hirman, J. W., G. R. Heckman, M. S. Greer, and J. B. Smith, "Solar and Geomagnetic Activity During Cycle 21 and Implications for Cycle 22," EOS, Vol. 69 (October 1988, pp. 962–972).

7. Kane, R. P., "Prediction of the Maximum Annual Mean Sunspot Number in the Coming Solar Maximum Epoch," *Sol. Phys.*, Vol. 108 (February 1987, p. 415).

8. Lantos, P. and P. Simon, "Prediction of the Next Solar Activity Cycle," *Proceedings of the 8th ESA Symposium on European Rocket and Balloon Programs and Related Research* (ESA SP-270) (1987, pp. 451–453).

9. Schatten, K. H., and S. Sofia, "Forecast of an Exceptionally Large Even–Numbered Solar Cycle," *Geophys. Res. Lett.*, Vol. 14 (June 1987, pp. 632–635).

10. Thompson, R. J., "The Rise of Solar Cycle 22," IPS TR–88–01, IPS Radio and Space Serv., Sydney (1988, 12 pp).

11. Akasofu, S.-I., "Energy Coupling Between the Solar Wind and the Magnetosphere," *Space Science Reviews*, Vol. 28 (February 1981, pp. 121–190).

12. Crooker, N. U., and G. L. Siscoe, "The Effect of the Solar Wind on the Terrestrial Environment," *Physics of the Sun*, Vol. 3, D. Reidel Publishing Company, Dordrecht, Holland (1986, pp. 193–249).

13. Basu, S., E. MacKenzie, and S. Basu, "Ionospheric Constraints on VHF/UHF Communications Links During Solar Maximum and Minimum Periods," *Radio Science*, Vol. 23 (May–June 1988, pp. 363–378).

14. Jasperse, J. R., "Sources and Characteristics of the Terrestrial Ionosphere," *Physics of Space Plasmas*, SPI Conference Proceedings and Reprint Series (Vol. 4, 1981, pp. 37–52).

15. Mendillo, M., J. A. Klobuchar, R. B. Fritz, A. V. da Rosa, L. Kersley, K. C. Yeh, B. J. Flaherty, S. Rangaswamy, P. E. Schmid, J. V. Evans, P. Schodel, D. A. Matoukas, J. R. Koster, A. R. Webster, and P. Chin, "Behavior of the Ionospheric F Region During the Great Solar Flare of August 7, 1972," *J. Geophys. Res.*, Vol. 79 (February 1974, pp. 665–672).

16. Baker, D. N., J. B. Blake, D. J. Gorney, P. R. Higbie, R. W. Klebesadel, and J. H. King, "Highly Relativistic Magnetospheric Electrons: A Role in Coupling to the Middle Atmosphere?," *Geophys. Res. Lett.*, Vol. 14 (October 1987, pp. 1027–1030).

17. Rosenbauer, H., H. Grunwaldt, M. D. Montgomery, G. Paschmann and N. Sckopke,"Heos 2 Plasma Observations in the Distant Polar Magnetosphere: The Plasma Mantle," *J. Geophys. Res.*, Vol. 80 (July 1975, pp. 2723–2737).

18. Hill, T. W., *Magnetospheric Boundary Layers*, ESA-SP-148, European Space Agency, Paris, p. 325.

19. DeForest, S. E., "Spacecraft Charging at Synchronous Orbits," *J. Geophys. Res.*, Vol. 77 (January 1972, pp. 561–569).

20. Mizera, P.F., and G. Boyd, "A Summary of Spacecraft Charging Results," *J. Spacecr. Rockets*, Vol. 20 (September–October 1983, pp. 438–443).

21. Vampola, A. L., "Thick Dielectric Charging on High-Altitude Spacecraft," *J. of Electrostatics*, Vol. 20 (January 1987, pp. 21–30).

22. Wenaas, E. P., "Spacecraft Charging Effects by the High Energy Natural Environment," *IEEE Trans. Nucl. Sci.*, NS–24 (1977, pp. 2281–2284).

23. Beers, B. L., "Radiation–Induced Signals in Cables," *IEEE Trans. Nucl. Sci.*, NS–24 (1977, pp. 2429–2434).

24. Hundhausen, A. J., *Coronal Expansion and Solar Wind*, Springer–Verlag, New York (1972, p. 135).

25. Hundhausen, A. J., *Coronal Holes and High Speed Streams*, Colorado Assoc. Univ. Press, Boulder (1977, p. 225).

26. Broussard, R. M., N. R. Sheeley, Jr., R. Tousey and J. H. Underwood, "A Survey of Coronal Holes and Their Solar Wind Associations Throughout Sunspot Cycle 21," *Solar Physics*, Vol. 56 (January 1978, p. 161–183).

27. Schulz, M.,"Interplanetary Sector Structure and the Heliomagnetic Equator," *Astrophys. Space Sci.*, Vol. 24 (October 1973, pp. 371–384).

28. Gonzalez, W. D., and B. T. Tsurutani, "Criteria of Interplanetary Parameters Causing Intense Magnetic Storms," *Planet. Space Sci.*, Vol. 35 (September 1987, pp. 1101–1109).

29. Gosling, J. T., J. R. Ashbridge, S. J. Bame, and W. C. Feldman, "Solar Wind Speed Variations: 1962–1974," *J. Geophys. Res.*, Vol. 81 (October 1976, pp. 5061–5070).

30. Crooker, N. U., J. Feynman, and J. Gosling, "On the High Correlation Between Long–Term Averages of Solar Wind Speed and Geomagnetic Activity," *J. Geophys. Res.*, Vol. 82 (May 1977, pp. 1933–1937).

31. Russell, C. T., "On the Possibility of Deducing Interplanetary and Solar Parameters from Geomagnetic Records," *Solar Phys.*, Vol. 42 (January 1975, pp. 259 -268).

32. Feynman, J., and S. M. Silverman,"Auroral Changes During the Eighteenth and Nineteenth Centuries and Their Implications for the Solar Wind and the Long–Term Variation of Sunspot Activity," *J. Geophys. Res.*, Vol. 85 (June 1980, pp. 2991–2997).

33. Schroder, W., "Aurorae During the Maunder Minimum," *Meteorol. Atmos. Phys.*, Vol. 38 (January 1988, pp. 246–251).

34. Silverman, S. M., "The Visual Aurora as a Predictor of Solar Activity," *J. Geophys. Res.*, Vol. 88 (October 1983, pp. 8123–8128).

35. Baker, D. N., L. F. Bargatze and R. D. Zwickl, "Magnetospheric Response to the IMF: Substorms," *J. Geomag. Geoelectr.*, Vol. 38 (October 1986, pp. 1047–1073).

36. Baker, D. N., R. D. Zwickl, S. J. Bame, E. W. Hones, Jr., B. T. Tsurutani, E. J. Smith and S. -I. Akasofu, "An ISEE 3 High Time Resolution Study of Interplanetary Parame-

ter Correlations With Magnetospheric Activity," *J. Geophys. Res.*, Vol. 88 (August 1983, pp. 6230–6242).

37. Snyder, C. W., Neugebauer, M., and U. R. Rao, "The Solar Wind Velocity and Its Correlation with Cosmic Ray Variations and Geomagnetic Activity," *J. Geophys. Res.*, Vol. 68 (December 1963, pp. 6361–6370).

38. Olbert, S., *Physics of the Magnetosphere*, D. Reidel Publishing Co., Dordrecht, Holland (1960, p. 641).

39. Garrett, H. B., Hassler, A. J., and T. W. Hill, "Influence of Solar Variability on Geomagnetic Activity," *J. Geophys. Res.*, Vol. 79 (November 1974, pp. 4603–4610).

40. Murayama, T., and K. Hakamada, "Effects of Solar Wind Parameters on the Development of Magnetospheric Substorms," *Planet. Space Sci.*, Vol. 23 (January 1975, pp. 75–91).

41. Maezawa, K., *Quantitative Modeling of Magnetospheric Processes*, American Geophysical Union, Washington, D. C. (1979, p. 436).

42. Murayama, T., *Magnetospheric Study 1979*, Japanese IMS Committee, Tokyo (1979, p. 296).

43. Feynman, J. and N. U. Crooker, "The Solar Wind at the Turn of the Century," *Nature*, Vol. 275 (October 1978, pp. 626–627).

44. Burton, R. K., R. L. McPherron and C. T. Russell, "An Empirical Relationship Between Interplanetary Conditions and Dst," *J. Geophys. Res.*, Vol. 80 (October 1975, pp. 4204–4214).

45. Hirshberg, J., "The Solar Wind Cycle, the Sunspot Cycle and the Corona," *Astrophys. Space Sci.*, Vol. 20 (1973, p. 473).

46. Mayaud, P. N., "Analysis of Storm Sudden Commencements for the Years 1868–1967," *J. Geophys. Res.*, Vol. 80 (January 1975, pp. 111–122).

47. Feynman, J., "Geomagnetic and Solar Wind Cycles: 1900–1975," *J. Geophys. Res.*, Vol. 87 (August 1982, pp. 6153–6162).

48. Gosling, J. T., J. R. Ashbridge and S. J. Bame, "An Unusual Aspect of Solar Wind Speed Variations During Solar Cycle 20," *J. Geophys. Res.*, Vol. 82 (August 1977, pp. 3311–3314).

49. Newton, H. W., "Sudden Commencements in the Greenwich Magnetic Records (1879–1944) and Related Sunspot Data," *Monthly Not. R. Astron. Soc.*, Vol. 5 (1948, 159–185).

50. Ohl, A. I., "Physics of the 11–Year Variation of Magnetic Disturbances," *Geomagn, Aeronomy*, Vol. 11 (1971, p. 549).

51. Neupert, W. M., and V. Pizzo, "Solar Coronal Holes as Sources of Recurrent Geomagnetic Disturbances," *J. Geophys. Res.*, Vol. 79 (September 1974, pp. 3701–3709).

52. Sheeley, N. R., Jr., and J. W. Harvey, "Coronal Holes, Solar Wind Streams and Geomagnetic Disturbances during 1977 and 1978," *Solar Phys.*, Vol. 70 (February 1981, pp. 237–247).

53. Feynman, J., "Implications of Solar Cycle 19 and 20 Geomagnetic Activity for Magnetospheric Processes," *Geophys. Res. Lett.*, Vol. 7 (November 1980, pp. 971–973).

54. Gleissberg, T., "The Eighty-Year Solar Cycle in Auroral Frequency Numbers," *J. Br. Astron. Assoc.*, Vol. 75 (January 1965, p. 227).

55. Akasofu, S.-I., "A Note on Variations of the IMF Bz and the AE Index Between 1966 and 1984 in Terms of Monthly and yearly Averages," *J. Geophys. Res.* (submitted, 1988).

56. King, J. H., "Solar Cycle Variations in IMF Intensity," *J. Geophys. Res.*, Vol. 84 (October 1979, pp. 5938–5940).

57. Yau, A. W., P. H. Beckwith, W. K. Petersen and E. G. Shelley, "Long-Term (Solar Cycle) and Seasonal Variations of Upflowing Ionospheric Ion Events at DE 1 Altitudes," *J. Geophys. Res.*, Vol. 90 (July 1985, pp. 6395–6407).

58. Collin, H. L., W. K. Petersen and E. G. Shelley, "Solar Cycle Variation of Some Mass Dependent Characteristics of Upflowing Beams of Terrestrial Ions," *J. Geophys. Res.*, Vol. 92 (June 1987, pp. 4757–4762).

59. Davies, K., "Ionospheric Radio Propagation," Monogr. 80, Natl. Bur. of Stand., Gaithersburg, Md. (1965).

60. Tascione, T. F., H. W. Kroehl, R. Creiger, J. W. Freeman, Jr., R. A. Wolf, R. W. Spiro, R. V. Hilmer, J. W. Shade, and B. A. Hausman, "New Ionospheric and Magnetospheric Specification Models," *Radio Science*, Vol. 23 (May–June 1988, pp. 211–222).

61. Lloyd, J. L., G. W. Haydon, D. L. Lucas, and L. R. Teters, "Estimating the Performance of Telecommunications Systems Using the Ionospheric Channel," in *Techniques for Analyzing Ionospheric Effects on HF Systems, Vol. 1,* Institute for Telecommunication Services, Boulder, Co. (1978).

62. Elkins, T. J., and C. M. Rush, "A Statistical Predictive Model of the Polar Ionosphere," Rep. AFCRL TR–0331, Air Force Cambridge Research Laboratory, Bedford, Ma. (1973).

63. Wakai, N., "Quiet and Disturbed Structure and Variations of the Nighttime E Region," *J. Geophys. Res.*, Vol. 72 (September 1967, pp. 4507–4517).

64. Gassman, G. J., "Analog Model 1972 of the Arctic Ionosphere," Rep. AFCRL TR–0305, Air Force Cambridge Research Laboratory, Bedford, Ma. (1973).

65. Vondrak, R. R., G. Smith, V. E. Hatfield, R. T. Tsunode, V. R. Frank, and P. D. Perreault, "Chatanika Model of the High–Latitude Ionosphere for Application to HF Propagation Prediction," Rep. 6056, RADC–TR–78–7, SRI Int., Menlo Park, Ca. (1978).

66. Wagner, R. A., "Modeling the Auroral E Layer," Rep. AFCRL TR–0305, Air Force Cambridge Research Laboratory, Bedford, Ma. (1972).

67. Mayaud, P. N., "Derivation, Meaning and Uses of Geomagnetic Indices," Geophysical Monograph 22, American Geophysical Union, Washington, D. C., (1980).

NOMENCLATURE

aa = 3-hour planetary geomagnetic index, derived from two antipodal stations

am = 3-hour (mondial) geomagnetic index

ap = 3-hour planetary geomagnetic index, derived from Kp

foE = critical frequency of the ionospheric E layer

foF_1 = critical frequency of the ionospheric F_1 layer

foF_2 = critical frequency of the ionospheric F_2 layer

hmE = altitude of the ionization peak in the ionospheric E layer

hmF_1 = altitude of the ionization peak in the ionospheric F_1 layer

n = solar wind density

AE = auroral electrojet index

AL = auroral electrojet index (lower envelope)

AU = auroral electrojet index (upper envelope)

B_x, B_y, B = Cartesian components of the interplanetary magnetic field

Dst = hourly geomagnetic index derived from midlatitude stations

Kp = 3-hour quasi-logarithmic planetary geomagnetic index

QE = effective 15-minute geomagnetic index

R = sunspot number

T = local time

V = solar wind speed

q = clock angle of the interplanetary magnetic field

SKp = 24-hour sum of Kp

c = solar zenith angle

Subscripts

a = auroral

o   = ordinary mode of radio propagation

p   = planetary

s   = solar

LABORATORY OPERATIONS

The Aerospace Corporation functions as an "architect-engineer" for national security projects, specializing in advanced military space systems. Providing research support, the corporation's Laboratory Operations conducts experimental and theoretical investigations that focus on the application of scientific and technical advances to such systems. Vital to the success of these investigations is the technical staff's wide-ranging expertise and its ability to stay current with new developments. This expertise is enhanced by a research program aimed at dealing with the many problems associated with rapidly evolving space systems. Contributing their capabilities to the research effort are these individual laboratories:

Aerophysics Laboratory: Launch vehicle and reentry fluid mechanics, heat transfer and flight dynamics; chemical and electric propulsion, propellant chemistry, chemical dynamics, environmental chemistry, trace detection; spacecraft structural mechanics, contamination, thermal and structural control; high temperature thermomechanics, gas kinetics and radiation; cw and pulsed chemical and excimer laser development, including chemical kinetics, spectroscopy, optical resonators, beam control, atmospheric propagation, laser effects and countermeasures.

Chemistry and Physics Laboratory: Atmospheric chemical reactions, atmospheric optics, light scattering, state-specific chemical reactions and radiative signatures of missile plumes, sensor out-of-field-of-view rejection, applied laser spectroscopy, laser chemistry, laser optoelectronics, solar cell physics, battery electrochemistry, space vacuum and radiation effects on materials, lubrication and surface phenomena, thermionic emission, photosensitive materials and detectors, atomic frequency standards, and environmental chemistry.

Electronics Research Laboratory: Microelectronics, solid-state device physics, compound semiconductors, radiation hardening; electro-optics, quantum electronics, solid-state lasers, optical propagation and communications; microwave semiconductor devices, microwave/millimeter wave measurements, diagnostics and radiometry, microwave/millimeter wave thermionic devices; atomic time and frequency standards; antennas, rf systems, electromagnetic propagation phenomena, space communication systems.

Materials Sciences Laboratory: Development of new materials: metals, alloys, ceramics, polymers and their composites, and new forms of carbon; nondestructive evaluation, component failure analysis and reliability; fracture mechanics and stress corrosion; analysis and evaluation of materials at cryogenic and elevated temperatures as well as in space and enemy-induced environments.

Space Sciences Laboratory: Magnetospheric, auroral and cosmic ray physics, wave-particle interactions, magnetospheric plasma waves; atmospheric and ionospheric physics, density and composition of the upper atmosphere, remote sensing using atmospheric radiation; solar physics, infrared astronomy, infrared signature analysis; effects of solar activity, magnetic storms and nuclear explosions on the earth's atmosphere, ionosphere and magnetosphere; effects of electromagnetic and particulate radiations on space systems; space instrumentation.